# Microphase Separation in Amorphous Polyethers Complexed with $LiClO_4$, $NaClO_4$, and NaI

**C. Vachon, M. Vasco, M. Perrier, and J. Prud'homme***

*Department of Chemistry, University of Montreal, Montreal, Quebec, Canada H3C 3J7*

*Received January 19, 1993; Revised Manuscript Received May 4, 1993*

ABSTRACT: Solubility and glass transition ($T_g$) data obtained for amorphous mixtures of $LiClO_4$ with poly(propylene oxide) (PPO) and poly(ethylene oxide) (PEO), both of molecular weights $4 \times 10^3$, confirm that cation–oxygen binding energy is of lower magnitude in PPO than in PEO. In agreement with anterior data reported by Moacanin and Cuddihy for a high molecular weight PPO, below a critical concentration, which corresponds to a molar ratio O/Li = 10 (O = ether oxygen), a liquid–liquid microphase separation takes place in the mixtures of the PPO–$LiClO_4$ system. A calorimetric analysis of the DSC data shows that more dilute mixtures of this system consist of microdomains of a fixed composition (O/Li = 10) in equilibrium with salt-free PPO. The same feature applies to the PPO–NaI system. Further data obtained on amorphous mixtures of PPO and PEO with $NaClO_4$ suggest that such a separation phenomenon, which is induced by the long-range Coulombic interactions, is probably a general feature of polyether electrolytes. Depending on the balance between these interactions and the cation–oxygen interactions, the complexed components in the present systems separate as either a macroscopic phase (PPO–$NaClO_4$) or a microphase (PPO–$LiClO_4$ and PPO–NaI) or as more discrete and more labile heterogeneities (PEO–$NaClO_4$).

## Introduction

Since the seminal paper by Armand *et al.*,[1] on the potential application of polyether–alkali metal salt complexes as thin-film, solid electrolytes in batteries, a considerable effort has been made to elucidate the physical basis of ion transport in these complexes.[2,3] In their optimal form, solid polyether electrolytes are rubbery materials that involve liquidlike molecular motion at the microscopic level. Their ionic conductivity exhibits a broad maximum over the concentration range $0.3 < c < 2$ mol/dm$^3$ in the concentrated regime. It is now well documented that the ion dynamics in such electrolytes is essentially governed by the segmental motion of the polymer host. However, besides this important feature, little is known about the thermodynamics of ion solvation in polyethers. Recent reports show that salt lattice energy is not the sole factor that governs solubility and its temperature dependence.[4,5] Other factors, such as the structure of the polymer, the geometry and the size of the ions, and the ion–ion interactions, appear to play a significant part in the balance that opposes salt lattice energy to cation–oxygen binding energy.

Previous data reported on solubility of NaSCN and KSCN in poly(ethylene oxide) (PEO), poly(methyl glycidyl ether) (PMGE), and poly(propylene oxide) (PPO) show features that suggest the formation of solvates of well-defined stoichiometries in the rubbery (or liquid) phases of the corresponding systems. In the first polymer (PEO),[4,6] solubility of these salts is temperature independent over a wide range of temperature, while in the second polymer (PMGE),[5] which has the same molecular formula as PEO, it exhibits discrete, step decreases with increasing temperature but remains unchanged on either side of these transitions. As reported by Teeters *et al.*,[7] in the third polymer (PPO), which has a lower density in oxygen atoms than PEO and PMGE, solubility of NaSCN and KSCN decreases markedly with increasing temperature. Salt precipitation occurs upon heating unsaturated mixtures of these systems. Seemingly, this feature, which also applies to NaI and $NaClO_4$ in PPO,[8] is difficult to interpret in terms of the chemical model proposed for the solvation of NaSCN and KSCN in the former two polyethers.[4,5] However, another feature related to the PPO–alkali metal salt systems concerns their phase behavior at low temperatures. As reported by Greenbaum *et al.*,[8] mixtures of PPO in a molar ratio O/Na = 8 (O = ether oxygen) with NaSCN and in a molar ratio O/Na = 16 with NaI both exhibit two glass transition ($T_g$) anomalies in their DSC curves. Such a feature had been reported over 25 years ago in the classical work by Moacanin and Cuddihy on the PPO–$LiClO_4$ system.[9] It suggests that a microphase separation takes place in the mixtures of these systems.

Contrary to NaSCN and KSCN, LiSCN dissolves in all proportions at its melting point ($T_m$ = 284 °C) in both PEO[10] and PMGE.[5] As reported in a recent work,[11] this feature also applies to $LiClO_4$ ($T_m$ = 251 °C) in PEO (PMGE was not studied). The solubility curves of LiSCN and $LiClO_4$ in PEO were constructed over wide ranges of temperature.[10,11] When these curves are analyzed in terms of the Flory–Huggins theory, they yield negative values for both the enthalpy and the entropy of mixing of the liquid components. From these thermodynamic data, a liquid–liquid phase separation is predicted to occur at a temperature well above the melting point of each salt.[10,11] Such a phase separation had already been visually observed above the melting point of the salt in mixtures of the PEO–KSCN ($T_m$ = 176 °C) system.[4] It is probably a general feature of polyether–salt systems at elevated temperatures. As the salt precipitation phenomenon reported for the PPO–NaX and PPO–KSCN systems[7,8] and as the step decreases in solubility reported for the PMGE–MSCN systems,[5] this feature results from the cost in entropy associated with salt solvation.

In view of the particular behavior of the PPO–alkali metal salt systems at low temperatures, it would be valuable to know more about the effect of the chemical structure of the polymer on the cation–oxygen binding energy, on the one hand, and on the entropy of solvation, on the other hand. A lithium salt such as $LiClO_4$, which is soluble in many polyethers including poly(1,3-dioxolane) and poly(tetrahydrofuran),[12] provides an opportunity to perform this kind of study. The present work focuses on the solubility behavior of this salt in a PPO sample having the same molecular weight ($M_n = 4 \times 10^3$) as the PEO sample used in the previous studies. The solubility curve

0024-9297/93/2226-4023$04.00/0 

constructed for this polymer is similar to that reported for PEO.[11] Its analysis allows the definition of the enthalpy and entropy of mixing of the liquid components. On the other hand, in agreement with the thermomechanical data reported by Moacanin and Cuddihy on comparable mixtures with a high molecular weight PPO,[9] the DSC data show that below a critical concentration, which corresponds to O/Li = 10, a microphase separation takes place in the PPO–$LiClO_4$ mixtures. A quantitative analysis of these data is presented at the beginning of this paper. It reveals that the stoichiometry of the complexed microphase is independent of the mixture compositions. This feature is corroborated by Raman spectral data reported by Torell and Schantz[13,14] on the same system.

Further data obtained on mixtures of PPO and PEO with $NaClO_4$ and NaI indicate that such a solvate–polymer separation, which is induced by the long-range Coulombic interactions, may take various forms depending on the nature of the salt and the polymer. Although a microphase separation also occurs for the PPO–NaI system, a macroscopic phase separation takes place in the mixtures of the PPO–$NaClO_4$ system. In turn, the $T_g$–composition relationship of the PEO–$NaClO_4$ system exhibits a singularity that suggests the formation of local, more labile complexed heterogeneities in PEO than in PPO. These features are interpreted in terms of a balance between the long-range Coulombic interactions, on the one hand, and the cation–oxygen interactions, on the other hand.

## Experimental Section

**Materials.** PPO and PEO samples were commercial polymers (Aldrich) with nominal molecular weights of $4 \times 10^3$. The PPO sample (a viscous liquid) was dried under high vacuum at 70 °C. The PEO sample (a crystalline solid) was dissolved in tetrahydrofuran (THF), precipitated in petroleum ether, and dried under high vacuum at room temperature. Both polymers were characterized by size exclusion chromatography (GPC) in THF by using a series of three Ultrastyragel columns with upper porosity limits of $10^2$, $5 \times 10^2$, and $10^3$ Å. The GPC analysis was made with a calibration curve constructed with low molecular weight PEO standards. The elution curve of the PPO sample was bimodal. A major (93% by weight), narrow peak centered at $M = 6.1 \times 10^3$ on the calibration scale was flanked by a minor (7% by weight), broad peak centered at $M = 1.5 \times 10^3$. In view of its low content, no attempts were made to remove the low molecular weight fraction. The global analysis yielded $M_n = 4.2 \times 10^3$ ($M_w/M_n = 1.35$) for the PPO sample compared to $M_n = 4.4 \times 10^3$ ($M_w/M_n = 1.02$) for the PEO sample.

$LiClO_4$ (K&K, 99.8%), $NaClO_4$ (Aldrich 99%), and NaI (Anachemia, reagent grade) were dried at 120 °C under high vacuum. Polymer–salt mixtures were prepared under a dry atmosphere by mixing weighed quantities of 1–5% methanol solutions of each component. Solvent evaporation was carried out in ampules connected to a vacuum system. The solvent-free mixtures were transferred into 25-mm-diameter, optically clear, glass vials with screw caps and dried under high vacuum for many days at room temperature. The mixtures containing $LiClO_4$ were further dried at 130 °C for a period of 24 h. The vials were stored under a dry atmosphere in a glovebox.

**DSC Measurements.** Glass transition anomalies were recorded at a heating rate of 40 °C/min. The calorimeter (Perkin-Elmer DSC-4) was flushed with dry helium. Supercooled specimens (with PEO) were obtained by melt quenching at a cooling rate of 320 °C/min. Values of $T_g$ were read at the intersection of the tangent drawn through the heat capacity jump with the base line recorded before the transition. Heat capacity increases, $\Delta c_p$, at $T_g$ were read at the temperature corresponding to the half-height of the transitions. Fusion and dissolution temperatures were read at the peak of the endotherms recorded at 10 °C/min. Sample pans were filled and sealed under a dry atmosphere in the glovebox.

**Optical Microscopy.** Temperatures corresponding to the onset of salt prescription (in the PPO–$NaClO_4$, PPO–NaI, and PEO–NaI mixtures) or to the end of salt dissolution (in the PPO–$LiClO_4$ mixtures), both upon heating at 10 °C/min, were monitored with a Zeiss polarizing microscope equipped with a programed hot stage (Mettler Model FP82). The specimens were placed between glass plates under a dry atmosphere, and the plates were transferred to the preheated hot stage by using a rubber-sealed drybox. NaI crystals, which are not birefringent, could be easily observed under unpolarized light as dark objects in a clear field.

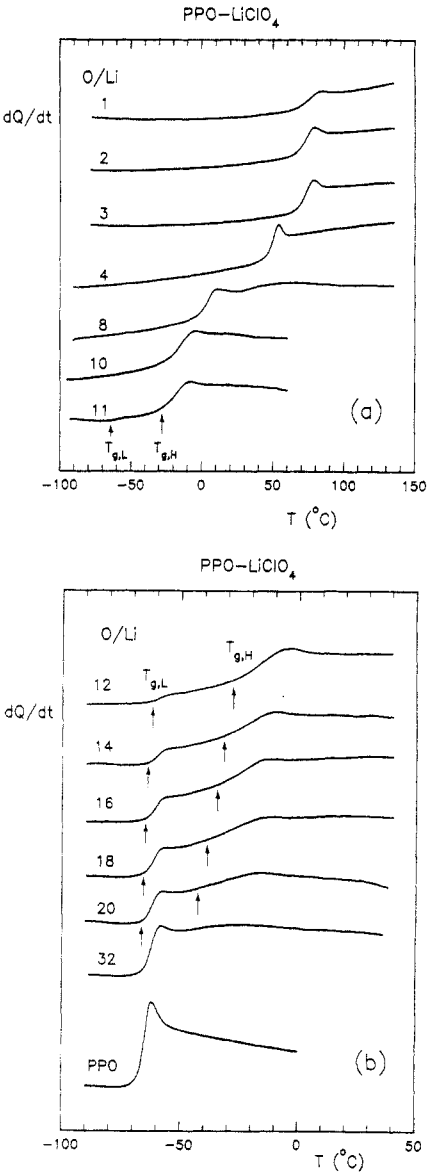


**Figure 1.** DSC heating curves recorded at 40 °C/min on mixtures of the PPO–$LiClO_4$ system. The mixtures with molar ratios O/Li over the range 11–20 exhibit two glass transition anomalies denoted as $T_{g,L}$ and $T_{g,H}$, respectively.

## Results and Discussion

**(a) Glass Transition Behavior of the PPO–Alkali Metal Salt Systems.** Figure 1 shows DSC curves recorded on PPO–$LiClO_4$ mixtures over the range O/Li = 1–32. All the mixtures with O/Li > 10 except the least concentrated mixture (O/Li = 32) exhibit two glass transition anomalies. Since these mixtures were optically clear and since there was no evidence for a two-layer macroscopic separation, this feature suggests the presence of a microphase having dimensions smaller than the wavelength of visible light. Judging by the value of $T_g$ (−64 °C) corresponding to the low-temperature anomaly in the O/Li = 11 mixture, a discrete microphase consisting of salt-free PPO first

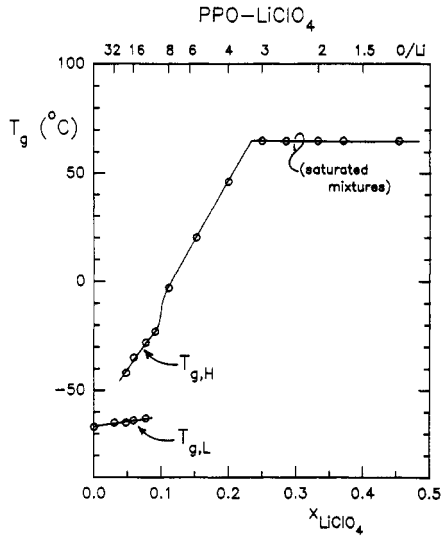


**Figure 2.** Plot of $T_g$ as a function of salt molar fraction for mixtures of the PPO–$LiClO_4$ system.

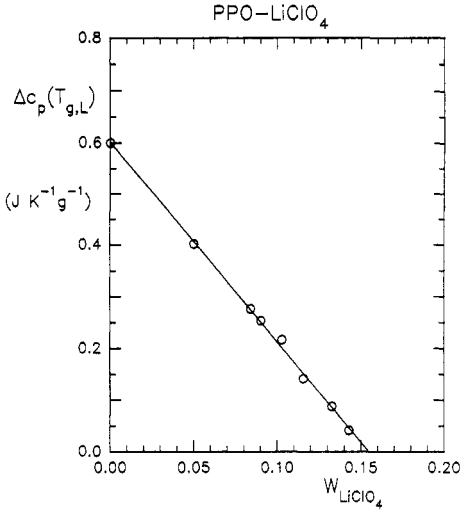


**Figure 3.** Plot of the heat capacity increase at $T_{g,L}$ ($\Delta c_p$, per gram of sample) as a function of salt weight fraction for mixtures of the PPO–$LiClO_4$ system.

separates with decreasing salt content. The $T_g$ of this microphase is 3 °C higher than that of salt-free PPO. This may be explained by considering that the discrete microdomains are dispersed in a rigid matrix and that some of their chains are anchored to this matrix. With further decrease in salt content, the low-temperature anomaly ($T_{g,L}$) increases in intensity and progressively shifts toward the value of $T_g$ of salt-free PPO. In turn, the high-temperature anomaly ($T_{g,H}$) decreases in intensity and exhibits a progressive spreading over the region above $T_{g,L}$.

These features are summarized in Figure 2, where the $T_g$ data corresponding to the onset of the transitions are plotted as a function of salt molar fraction ($x_{salt}$). Although these features are comparable to those reported by Moacanin and Cuddihy[9] for a high molecular weight PPO, they are at variance with those reported by McLin and Angell[15] for a PPO of the same molecular weight as the present PPO. In that latter study, however, only one composition (O/Li = 16) was examined over the range where two glass transitions are observed in the present work. Since the DSC curve reported for this composition did not exhibit this feature, DSC measurements were performed by applying the same heating rate (10 °C/min instead of 40 °C/min) as that quoted by McLin and Angell.[15] Further measurements were also made at both heating rates on specimens (O/Li = 16 and 18) prepared with the same solvent (acetonitrile instead of methanol) as that quoted by these authors. Although, as expected, the slower heating rate yielded a systematic $T_g$ shift of −3 °C, these DSC curves were fully consistent with those depicted in Figure 1.

The features related to $T_{g,L}$ and $T_{g,H}$ in Figure 1 are reminiscent of those reported for mesomorphic block polymers involving soft and hard microphases.[16] In such materials, the vitrification of the hard microphase occurs in a situation where both microphases are liquidlike. Due to the dynamical interactions that take place at the microdomain boundary, the chain segments near the interface are immobilized at a lower temperature than those in the core of the microphase. In turn, the vitrification of the soft microphase occurs in a situation where the hard microphase is already frozen. In this situation, it is essentially the anchorage of the chains to the rigid microphase that affects their vitrification process. In other words, there is no extensive transfer of kinetic energy from one microphase to the other as in the former situation. Since a similar cascade of events takes place upon the subsequent heating of the material, a considerable spreading of $T_{g,H}$ may occur, particularly for materials in which the hard microphase is highly dispersed, that is, with a high surface to volume ratio. At the limit, as probably happens for O/Li > 20 in Figure 1, this spreading becomes substantial enough to make it difficult (or impossible) to detect $T_{g,H}$ by DSC.

In view of these considerations, a quantitative analysis of the DSC curves must focus on $T_{g,L}$ rather than on $T_{g,H}$. As a rational basis for such an analysis, it may be postulated that the heat capacity increase, $\Delta c_p$, at $T_{g,L}$ (per gram of sample) is a measure of the weight fraction of the salt-free microphase in the mixtures. A plot of this quantity is depicted in Figure 3 as a function of salt weight fraction ($W_{salt}$). This plot yields a linear curve that extrapolates to $W_{salt} = 0.154$ (O/Li = 10.1) at a zero value of $\Delta c_p$. Such a linear plot reveals that the composition of the complexed microphase is independent of the global salt content of the mixtures. This feature also applies to the least concentrated mixture (O/Li = 32). Although the glass transition related to its complexed microphase is not apparent in the DSC curve, this microphase still contributes to a finite proportion of the material. Indeed, according to the data in Figure 3, its weight fraction is 33% compared to 54% for the O/Li = 20 mixture. This suggests a structure consisting of discrete microdomains dispersed in a PPO matrix. As judged from the changes in the DSC curves of Figure 1, with increasing salt content these microdomains first increase in number and then progressively fuse together to form a continuous microphase.

Among the previous studies on the PPO–$LiClO_4$ system, special attention should be paid to that reported by Torell and Schantz.[13,14] In this study, an analysis of Raman spectra obtained over the range O/Li = 5–1000 yields stunning results concerning the degree of dissociation of $LiClO_4$ in a PPO of the same molecular weight as the present PPO. According to this analysis, which is based on a two-component band related to the symmetric stretching mode of the perchlorate anion, the degree of dissociation ($\alpha$) of $LiClO_4$ would remain invariant, ca. 87% (at 22 °C) over the range O/Li = 10–1000 (i.e., from $c$ = 0.02 to $c$ = 1.6 mol/dm$^3$).[14] For higher concentrations, $\alpha$ would decrease markedly to reach the value of 55% at $c$ = 2.9 mol/dm$^3$ (O/Li = 5). These features are in conflict with conductivity data reported for the same salt in ether solvents of comparable dielectric constant.[17] In these

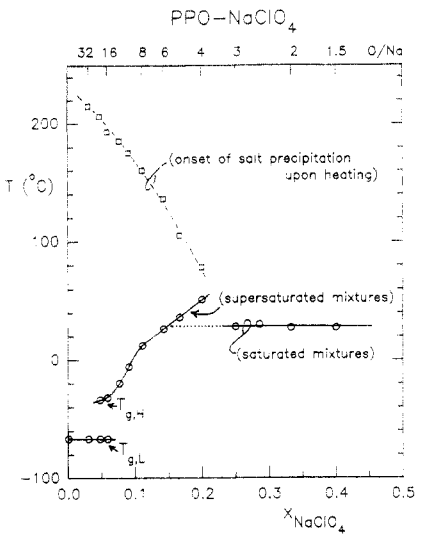


**Figure 4.** Plots of $T_g$ (circles) and temperatures corresponding to the onset of salt precipitation (squares) as a function of salt molar fraction for mixtures of the PPO–$NaClO_4$ system.

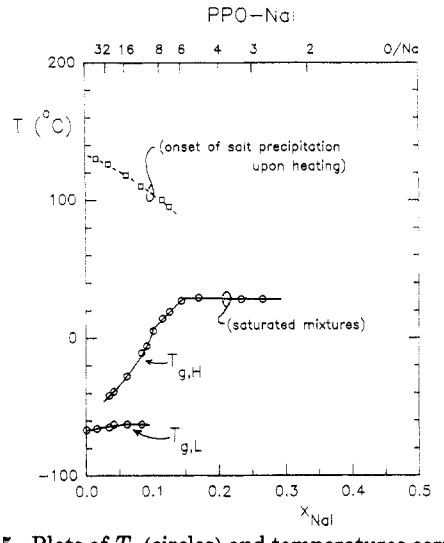


**Figure 5.** Plots of $T_g$ (circles) and temperatures corresponding to the onset of salt precipitation (squares) as a function of salt molar fraction for mixtures of the PPO–NaI system.

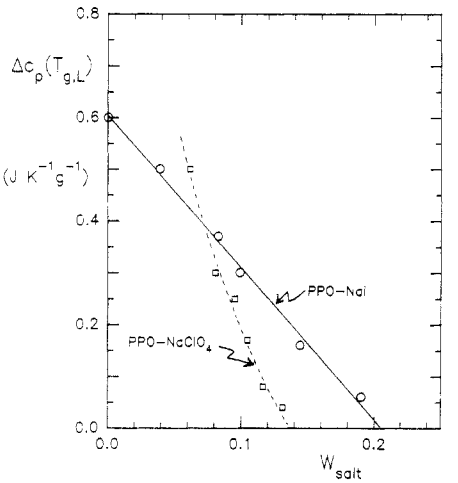


**Figure 6.** Plots of the heat capacity increase at $T_{g,L}$ ($\Delta c_p$, per gram of sample) as a function of salt weight fraction for mixtures of the PPO–NaI system (circles) and the PPO–$NaClO_4$ system (squares).

solvents, as well as in PEO oligomers[18] and copolymers,[19] the concentration dependence of molar conductivity exhibits a minimum over the range $c$ = 0.01–0.03 mol/dm$^3$ that suggests a sizable association at the lower end of the concentration range studied by Torell and Schantz.

When the spectral data reported by these authors are interpreted on a more general basis, that is, without any specific reference to ion association, they simply show that the anion environment remains unchanged below a critical concentration that corresponds to O/Li = 10, approximately. Not only is this feature consistent with the present data, but it also reveals that $LiClO_4$ is confined to microdomains of 10/1 stoichiometry over a wide range of concentrations in the dilute regime. Furthermore, it reveals that the microphase separation is not induced by the cooling process associated with the $T_g$ measurements. Interestingly, the Raman bands related to the symmetric stretching mode of the $SO_3$ group in PPO–$NaCF_3SO_3$ mixtures exhibit a similar trend.[13,14] Since their relative intensities were reported to remain unchanged for O/Na > 16 in a comparable series of mixtures (O/Na = 5–1000), it may be argued that a microphase of invariant composition also forms for $NaCF_3SO_3$ contents inferior to this limit. This feature is in part substantiated by DSC data reported by McLin and Angell on a limited number of compositions related to this system.[15] Mixtures with O/Na = 30 and 40 both exhibited a $T_g$ elevation of 4 °C with respect to salt-free PPO, while the next composition studied by these authors (O/Na = 16) exhibited a $T_g$ elevation of 22 °C.

Figure 4 shows $T_g$ data obtained for mixtures of the PPO–$NaClO_4$ system. These data, which correspond to measurements performerd a few days after the mixture preparation, exhibit features roughly similar to those depicted in Figure 2 for the PPO–$LiClO_4$ system. Nevertheless, over a period of 1–2 weeks a turbidity developed in the mixtures with O/Na > 14, and over a longer time, a two-layer macroscopic separation could be observed in these mixtures. Special attention was paid to the mixture with O/Na = 32, which exhibited a single $T_g$ (−67 °C) a few days after its preparation. The upper layer was a clear material having a $T_g$ of −67 °C. The lower layer was a turbid material of higher viscosity having two $T_g$'s ($T_{g,L}$ = −67 °C and $T_{g,H}$ = −35 °C). Note that its value of $T_{g,H}$ is essentially the same as those of the more concentrated mixtures with O/Na = 16 and 20 in Figure 4. Also note that contrary to the PPO–$LiClO_4$ system (Figure 2), there is no perceptible elevation of $T_{g,L}$ with respect to salt-free PPO for the mixtures with O/Na > 16 in Figure 4. This suggests that just after their preparation the mixtures containing $NaClO_4$ were composed of larger salt-free microdomains than those containing $LiClO_4$. The fact that these microdomains, which had formed upon the solvent casting process, were prone to coalesce is puzzling. It is not due to the lower charge density of the cation since, as will be shown shortly, this feature does not apply to the PPO–NaI system.

As depicted in Figure 5, the $T_{g,L}$ and $T_{g,H}$ data related to the PPO–NaI system are comparable to those of the PPO–$LiClO_4$ system. With increasing salt content, $T_{g,L}$ exhibits a progressive shift to reach an elevation of 4 °C with respect to salt-free PPO. Figure 6 shows the calorimetric diagram ($\Delta c_p$ vs $W_{salt}$) associated with this transition. This diagram yields a linear curve that extrapolates to $W_{salt}$ = 0.205 (O/Na = 10.0) at a zero value of $\Delta c_p$. Included in Figure 6 is a similar diagram constructed for the PPO–$NaClO_4$ system. It may be seen that, although the curve of this diagram extrapolates to $W_{salt}$ = 0.135 (O/Na = 13.5) at a zero value of $\Delta c_p$, it fails to extrapolate to the value of $\Delta c_p$ of salt-free PPO at a zero value of $W_{salt}$. This inconsistency reveals that sedimen-

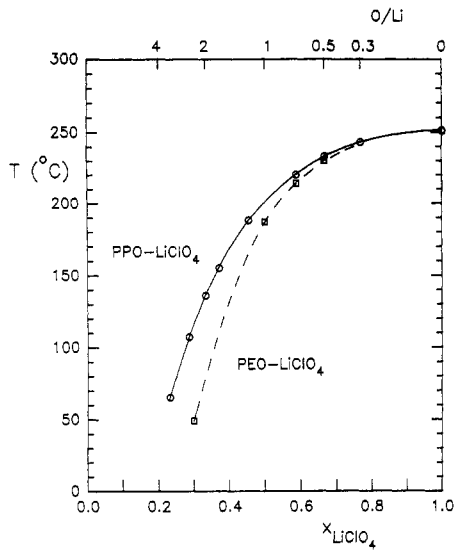


**Figure 7.** Temperature–composition diagram depicting the solubility curves for $LiClO_4$ in PPO (circles) and PEO[11] (squares). The right ordinate, which is common to both systems, corresponds to the melting point of the salt. Complete miscibility occurs over a range of temperature above each curve.

tation had already occurred a few days after the preparation of the mixtures containing this salt.

**(b) Solubility Behavior of $LiClO_4$ in PPO and PEO.** Figure 7 shows a comparison made on a molar basis of the solubility curves of $LiClO_4$ in PPO and PEO, respectively. In either case, the data point at the lowest temperature (65 °C for PPO and 49 °C for PEO) corresponds to the solubility derived from the ceiling value of $T_g$ in the $T_g$–composition relationship (Figure 2 for PPO and Figure 10 for PEO). The other data were obtained by means of microscopy (PPO, O/Li > 1) or DSC measurements performed at a heating rate of 10 °C/min. Microscopy was used to confirm that the sharp endotherms recorded by DSC were positively associated with the end of salt dissolution.

Apart from the fact that $LiClO_4$ is soluble in all proportions at elevated temperatures in both polymers and that on a molar basis its solubility is greater in PEO than in PPO at moderate temperatures, little information can be obtained from a simple inspection of the data depicted in Figure 7. However, a thermodynamic analysis of these data, which are the analogue of the melting point depression of the salt by the polymer diluent, can yield quantitative information on the interaction enthalpy and entropy between the components of these systems. Such information, if derived from an adequate theory, may help to understand why a microphase separation occurs in PPO but not in PEO. As shown in a former work[11], the Flory–Huggins lattice theory for polymer–solvent free energy of mixing provides a useful approach to approximate these thermodynamic quantities. Note that an analysis with more sophisticated theories, such as those involving a free volume contribution to the free energy of mixing, would require complementary data on volumic properties that are unknown at this time. According to the results obtained in the former work on PEO,[11] it is likely that the interactional contribution is dominant in the present systems.

In terms of the lattice theory, the melting point depression of the salt (denoted by the subscript s) by the polymer diluent (denoted by the subscript p) should be governed by the magnitude of the familiar Flory–Huggins

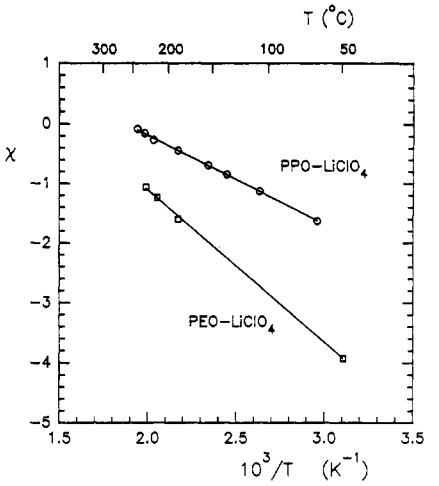


**Figure 8.** Plots as a function of $1/T$ of the Flory–Huggins interaction parameter $\chi$ derived from the solubility data of $LiClO_4$ in PPO (circles) and PEO (squares). These relationships can be represented by eqs 6 and 7, respectively.

$\chi$ parameter according to the relation[20]

$$\frac{1}{T_m} - \frac{1}{T_m^\circ} = -\frac{R}{\Delta H_{f,s}}\left[\ln(1-\varphi_p) + \left(1-\frac{1}{x}\right)\varphi_p + \chi\varphi_p^2\right] \quad (1)$$

where $\Delta H_{f,s}$ is the molar heat of fusion of the salt, $\varphi_p$ is the volume fraction of the polymer, $x$ is the number of segments per chain having the same partial molar volume as that of the salt ($V_s$), and $R$ is the ideal gas constant.

The parameter $\chi$ in eq 1 is a measure of the excess free energy of mixing, $\Delta G_{M,e}$, of the liquid components. When this latter quantity is written per unit of volume of mixture (denoted by the superscript v), it is given by the relation[20]

$$(\Delta G_{M,e})^v = RT\chi\varphi_p(1-\varphi_p)/V_s \quad (2)$$

By assuming that $\chi$ is composition independent and changes with temperature according to the simple relation

$$\chi = a/T + b \quad (3)$$

eq 2 can be divided into enthalpic and entropic terms:

$$(\Delta H_{M,e})^v = Ra\varphi_p(1-\varphi_p)/V_s \quad (4)$$

$$(\Delta S_{M,e})^v = -Rb\varphi_p(1-\varphi_p)/V_s \quad (5)$$

Figure 8 shows plots as a function of $1/T$ of the values of $\chi$ obtained by applying eq 1 to the solubility data of $LiClO_4$ in PPO and PEO, respectively. The values of $\varphi_p$ were estimated from the weight fractions by assuming that the density ratio $\rho(LiClO_4)/\rho(\text{polymer})$ was temperature independent and close to that of the crystalline components at 25 °C; that is, $\rho(LiClO_4) = 2.43$ g/cm³, $\rho(\text{PPO}) = 1.13$ g/cm³ (isotactic form), and $\rho(\text{PEO}) = 1.23$ g/cm³. As estimated from the same density ratio, the values of $x$ were 80 for PPO and 72 for PEO, and as measured by DSC the value of $\Delta H_f(LiClO_4)$ was 14.6 kJ/mol. In agreement with eq 3, both polymers yield linear plots of $\chi$ as a function of $1/T$. The corresponding analytical expressions are

$$\chi = (-1.50 \times 10^3/T) + 2.80 \quad \text{(for PPO)} \quad (6)$$

and[11]

$$\chi = (-2.56 \times 10^3/T) + 4.00 \quad \text{(for PEO)} \quad (7)$$

These relationships show that the magnitudes of both the interaction enthalpy (favorable to mixing) and the interaction entropy (unfavorable to mixing) are less in PPO than in PEO. As a first step in the interpretation of these results, it may be postulated that two distinct

effects play significant but opposite parts in the interaction enthalpy. The first of these effects, which is the dominant one, is the exothermic contribution resulting from the cation–oxygen binding energy. The second effect is related to the ion–ion Coulombic energy. Since the presence of the polymer contributes to increase the average distance between the ions, this effect is necessarily endothermic. Furthermore, for a given ratio O/Li near the saturation composition, this unfavorable effect should be greater for PPO because this polymer has a lower density in oxygen atoms than PEO ($\varphi_p$ is greater for PPO than for PEO). Therefore, at this point, it is difficult to discriminate between a lower binding energy and a Coulombic effect, or both, as the cause of the lower interaction enthalpy related to PPO. Fortunately, a partial answer to this question can be found in the phase behavior at low salt contents.

**(c) Binding Energy and Solvate Structure at Low Salt Contents.** The microphase separation in the PPO-rich mixtures indicates that a uniform dispersion of the salt is possible only if ion concentration is greater than a critical value. Below this critical value, the salt dispersion rearranges into a more stable microscopic structure involving local regions with a higher concentration in ions. This occurs because Coulombic energy is liberated through this process. In other words, the complexed microdomains are stabilized by the long-range ion–ion interactions. Their formation, however, depends on the balance between these interactions and the cation–oxygen interactions. This is particularly true at low temperatures where the free energy of mixing of the liquid components is dominated by the interaction enthalpy. In such a situation and in the absence of long-range ion–ion interactions, the cation–oxygen interactions (if sizable enough to favor dissolution) would necessarily yield a uniform dispersion of the salt. Thus, it is founded to argue that for a given salt in different polyethers, microdomain formation takes place only when cation–oxygen binding energy is lower than a critical value. In turn, it may be argued that for different salts in a given polyether, it takes place only when the complexed microdomains can involve Coulombic energy superior to a critical value.

Microdomain composition and microdomain size are two other variables that should play an important role in this process. Although the microdomain composition probably corresponds to a well-defined stoichiometry involving a maximum of interactions with a minimum of internal tension, the microdomain size is a more complex variable. This variable, which governs the magnitude of the interfacial area between the salt-free regions and the complexed regions, should further adjust to minimize the free energy of the mixture. These considerations may provide an explanation of the macroscopic separation observed in the mixtures of the PPO–$NaClO_4$ system. The long-range Coulombic interactions are stronger in this system than in the PPO–NaI system. As will be shown shortly, this feature is substantitated by the greater stability of the PPO–$NaClO_4$ mixtures at elevated temperatures. Stronger long-range Coulombic interactions within the complexed microdomains necessarily mean a greater cost in free energy associated with the interfacial area. Note that a similar but inverse argument may be applied in terms of the binding energy. In turn, in a situation with either weaker long-range Coulombic interactions or greater binding energy, the complexed microphase may possibly reduce to the level of local, more labile heterogeneities.

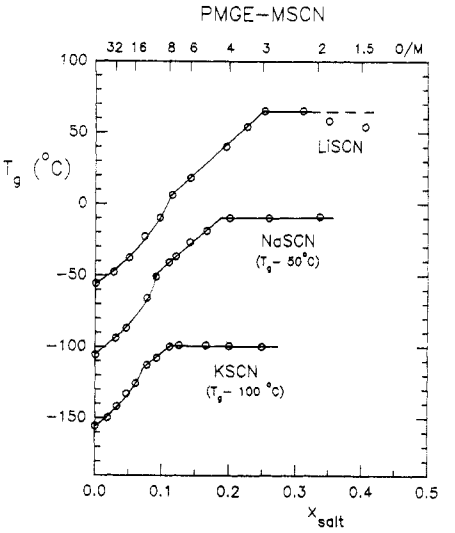


**Figure 9.** $T_g$–composition relationships of the PMGE–MSCN (M = Li, Na, K) systems.[5]

PMGE provides an example of a polymer in which such heterogeneities appear to form at low salt contents. Evidence for this feature may be found in the $T_g$–composition relationships reported in a former work on mixtures of this polymer with LiSCN, NaSCN, and KSCN.[5] As illustrated in Figure 9, with increasing salt content the $T_g$ data of these systems first exhibit an accelerated rise up to a critical concentration and then adopt a linear relationship up to saturation. Although none of the mixtures exhibited two $T_g$ anomalies, it may be seen that the changes of regime occur at molar ratios comparable to those of the present systems, that is, O/Li = 8, O/Na = 10, and O/K = 13, respectively.

In the former work devoted to PMGE,[5] these critical compositions were tentatively attributed to the completion of a solvation process involving a preferential binding with either the pendant groups or the chain backbone of PMGE. In view of the phase behavior of the PPO systems, it may now be argued that the initial, accelerated rise in $T_g$ rather results from an increasing amount of discrete heterogeneities having a greater salt content than the nominal composition of the mixtures. Like the complexed microdomains in PPO, they probably correspond to local, solvated entities having a fixed composition. The difference, however, is that the mixtures containing these heterogeneities appear as homogeneous mixtures upon the time scale of the $T_g$ measurements made by DSC. This feature indicates that, presumably due to a greater binding energy in PMGE, these local fluctuations rearrange at a rate considerably greater than that of the microdomains in PPO.

$T_g$ data previously reported[4] for supercooled mixtures of PEO with LiSCN and KSCN yielded linear $T_g$–composition relationships from O/M = 32 (the lowest salt content examined) up to saturation (O/M = 3 for LiSCN and O/M = 5 for KSCN). A similar, linear relationship was also reported[5] for supercooled mixtures of NaSCN with a P(EO/MGE) random copolymer containing 10 mol % of MGE units. Although the $T_g$ of salt-free PEO cannot be measured directly by DSC,[21] these relationships extrapolated to the same value of $T_g$ (−67 °C) at a zero value of $x_{salt}$. In more recent works,[11,22] $T_g$ data over wide ranges of compositions were reported for three other PEO–LiX systems (X = $ClO_4^-$, $CF_3SO_3^-$, and $N(CF_3SO_2)_2^-$). As illustrated in Figure 10 for $LiClO_4$, these data also extrapolated to the value of −67 °C at a zero value of $x_{salt}$. None of the corresponding relationships exhibited an

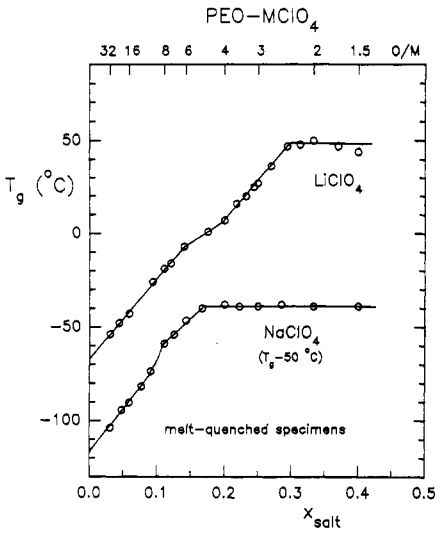


**Figure 10.** $T_g$–composition relationships of the PEO–$LiClO_4$ and PEO–$NaClO_4$ systems. The data correspond to supercooled mixtures.

accelerated rise over the composition range $6 < O/Li < 32$. At higher salt contents ($O/Li < 6$), a singularity (other than that due to saturation) was observed for $LiClO_4$ only. As may be seen in Figure 10, it corresponds to a sharp translation of the linear relationship along the composition axis. This effect, which suggests a structural rearrangement, is different from that observed for the PMGE–MSCN systems (Figure 9).

Figure 10 also shows the $T_g$–composition relationship obtained for supercooled mixtures of $NaClO_4$ with PEO. It may be seen that this system exhibits the same singularity as the PMGE–MSCN systems. A change of regime occurs at a molar ratio $O/Na = 8$. Attempts were made to obtain $T_g$ data over the same range of compositions with NaSCN and NaI. Unfortunately, only the mixtures with $8 < O/Na < 32$ could be successfully supercooled by melt quenching. Over this limited range of compositions, the $T_g$ data related to these salts were essentially the same as those of $NaClO_4$. Note that NaSCN,[6] NaI, and $NaClO_4$ form 3/1 (O/Na) crystalline compounds with PEO that melt incongruently at 182, 175, and 144 °C, respectively (phase diagrams of the PEO–$NaClO_4$ and PEO–NaI systems are depicted in Figures 11 and 12). The difficulty encountered to inhibit the crystallization of the former two compounds is apparently associated with their higher melting temperatures.

The singularity in the $T_g$–composition relationship of the PEO–$NaClO_4$ system is not as marked as that in the relationship of the PMGE–NaSCN system. This suggests that the heterogeneities are of smaller size in PEO than in PMGE. In addition, it is clear that if the size of these heterogeneities had been inferior to this limit, their presence could not have been detected by $T_g$ measurements. In view of the singularity observed for the PEO–$NaClO_4$ system, it is likely that such heterogeneities exist in the other PEO electrolytes. Dynamic thermomechanical analysis,[9] or even vibrational molecular spectroscopy, if not biased by features resulting from ion association, would be more appropriate to investigate this matter.

**(d) Solubility Behavior of $NaClO_4$ and NaI in PPO and PEO.** The temperature–composition relationships related to the onset of salt precipitation in unsaturated mixtures of the PPO–$NaClO_4$ and PPO–NaI systems are depicted in Figures 4 and 5, respectively. It may be seen that these relationships (dashed curves) do not extrapolate to the same solubility limit at low temperatures as that

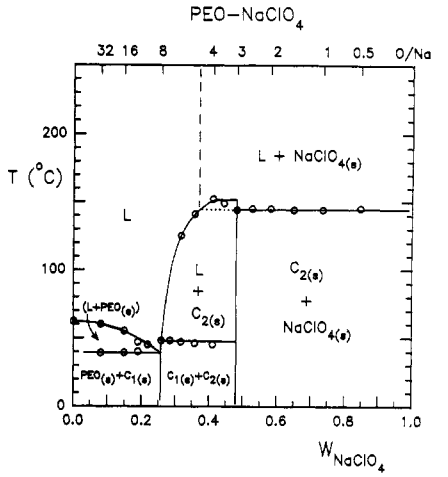


**Figure 11.** Phase diagram of the PEO–$NaClO_4$ system. The vertical boundaries at $W_{salt} = 0.26$ and 0.48 were derived from a calorimetric analysis of the DSC data. They show the formation of 8/1 and 3/1 crystalline compounds designated by $C_{1(s)}$ and $C_{2(s)}$, respectively. Over the range 150–300 °C, salt was absent for O/Na = 5 but present for O/Na = 4. Thus, the dashed line at $W_{salt} = 0.37$ (O/Na = 4.7) may be considered as a good approximation of the salt liquidus curve over this range.

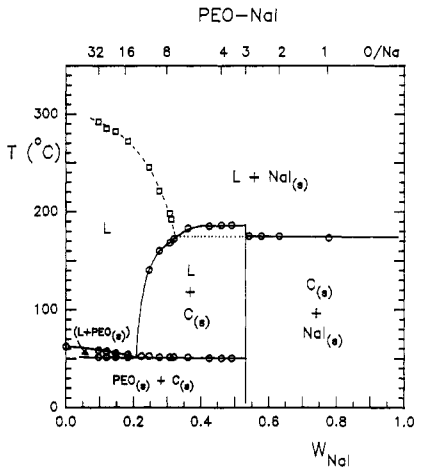


**Figure 12.** Phase diagram of the PEO–NaI system. The vertical boundary at $W_{salt} = 0.53$ was derived from a calorimetric analysis of the DSC data. In agreement with anterior data on this system,[2] this boundary shows the formation of a 3/1 crystalline compound designated by $C_{(s)}$. The dashed curve above the melting point of this compound corresponds to the onset of salt precipitation defined by microscopy.

(O/Na = 6 at 28 °C) derived from the ceiling values of $T_g$ of these systems. This indicates that upon heating salt precipitation was retarded due to a supersaturation phenomenon. Furthermore, as quoted in Figure 4, some of the PPO–$NaClO_4$ mixtures (O/Na = 4 and 5) were already supersaturated in their as-cast, vitreous form. Their values of $T_g$ are greater than those of the more concentrated mixtures that were positively defined as saturated mixtures by visual inspection.

In spite of this supersaturation effect, it is clear that at elevated temperatures solubility of $NaClO_4$ in PPO is much greater than that of NaI. For instance, in mixtures with composition O/Na = 8 onset of precipitation occurs at 160 °C for $NaClO_4$ compared to 100 °C for NaI. This difference is not due to the lower lattice energy of $NaClO_4$ (648 kJ/mol compared to 704 kJ/mol for NaI)[23] since both salts exhibit the same solubility limit (O/Na = 6) at low temperatures. It is probably due to the presence of stronger long-range Coulombic interactions in the liquid phase containing the perchlorate anion. This explanation is consistent with the foregoing interpretation of the

macroscopic, liquid–liquid separation that takes place in the PPO-rich mixtures with $NaClO_4$.

Inspection of the phase diagrams of the PEO–$NaClO_4$ and PEO–NaI systems (Figures 11 and 12) shows that a supersaturation phenomenon also takes place in PEO. It concerns the peritectic reaction associated with the incongruent melting of the 3/1 intermediate compound. As in the PEO–NaSCN system,[6] this reaction occurs because salt solubility is inferior to the salt content of the 3/1 compound. However, a true peritectic equilibrium is observed only for the mixtures with O/Na < 3, that is, those mixtures that contained solid salt prior to their melting. This equilibrium is defined by the horizontal tie line at 144 °C for the PEO–$NaClO_4$ system, and that at 175 °C for the PEO–NaI system. Salt solubility at these temperatures may be obtained by extrapolating this tie line to the solubility curve of the 3/1 compound.[6] It corresponds to O/Na = 4.7 for $NaClO_4$ and to O/Na = 7.4 for NaI. Note that the latter result is consistent with the temperature–composition relationship related to NaI precipitation in PEO (Figure 12).

According to the $T_g$–composition relationship in Figure 10, solubility of $NaClO_4$ in PEO corresponds to O/Na = 5 at 11 °C (the ceiling value of $T_g$). Furthermore, as could be judged by microscopy, above the peritectic equilibrium (144 °C) it remains within the range 4 < O/Na < 5 up to 300 °C (the upper temperature examined). This feature suggests that the solubility of this salt in PEO, like that of NaSCN, is governed by the formation of a solvate of well-defined stoichiometry. On the other hand, the marked decrease in the solubility of NaI at elevated temperatures confirms that weaker long-range Coulombic interactions are associated with this salt.

## Concluding Remarks

This study clearly shows that the long-range Coulombic interactions play a determinant role on the phase behavior of polyether amorphous electrolytes. Not only are these interactions responsible for the liquid–liquid phase separation that takes place in PPO electrolytes, but with other factors they also govern the solubility behavior of alkali salts in polyethers. This point may be illustrated by summarizing some features related to PEO. Although $LiClO_4$ and LiSCN are soluble in all proportions at elevated temperatures in this polymer, over a wide range of temperature solubility of $NaClO_4$, as well as that of the other alkali metal thiocyanates (from NaSCN to CsSCN),[4-6] is temperature independent. Phase diagrams recently reported for the PEO–alkali metal triflate systems[22] show that this latter feature applies to $CsCF_3SO_3$ but not to the other alkali metal triflates. The latter salts (from $LiCF_3SO_3$ to $RbCF_3SO_3$) are soluble in all proportions at elevated temperatures in PEO. These data for various salts indicate that above a critical size of the cation, which depends on the nature of the anion, solubility is governed by the formation of a solvate of well-defined stoichiometry. This feature may be explained by considering that with increasing salt concentration in the concentrated regime the non-Coulombic interactions favorable to dissolution can be overwhelmed by the long-range Coulombic interactions. This situation may give rise to another separation phenomenon due to the Coulombic interactions, that is, the separation of a solvate from the salt. If this solvate is stable over a wide range of temperature and if the balance remains unchanged over this range, solubility will also remain unchanged as is the case for a limited number of salts in PEO.

As shown in the previous works on PEO and PMGE,[4-6] the stoichiometry of the solvate that separates from the salt at low temperatures is governed by the geometry and the size of the ions. It is likely that this feature also applies to the lithium salts.[5] However, due to the great polarizing power of $Li^+$, the interactional balance probably changes in favor of the non-Coulombic interactions with increasing temperature. This would explain why the solubility of LiSCN and $LiClO_4$ exhibits a classical relationship at elevated temperatures. A similar effect may explain the solubility behavior of the alkali metal triflates in PEO. All these salts except $CsCF_3SO_3$ form 1/1 crystalline compounds with this polymer.[22] Furthermore, in the case of $NaCF_3SO_3$ and $KCF_3SO_3$, the melting points of these compounds are higher than those of the salts. This suggests that the triflate anion may contribute to further non-Coulombic interactions that are favorable to salt dissolution at elevated temperatures.

Another point concerns the effect of the chemical structure of PPO on the conductivity magnitude of its electrolytes with alkali metal salts. For mixtures in a molar ratio O/Na = 8, which correspond to homogeneous solutions of the present salts ($LiClO_4$, $NaClO_4$, and NaI), the $T_g$ elevations produced in PPO are 25–30% greater than those in PEO. Note that salt-free PPO has the same value of $T_g$ as salt-free PEO. This latter feature is essentially due to the C–C–O bonds in the repeat units of these polymers. Thus, in the presence of bare oxygen atoms, the methyl substituent on the PPO repeat unit has no perceptible effect on the chain stiffness. When cation–oxygen binding takes place, however, this substituent produces a considerable hindrance to bond rotation. Since binding energy is not as great in PPO as in PEO, it is probably this steric effect that accounts for the greater $T_g$ elevations in PPO.

According to the current views on polyether electrolytes,[2,3] a lower binding energy is expected to be favorable to cation mobility. In turn, a greater $T_g$ elevation, which means a lower free volume or a lower kinetic energy at a given temperature, is unfavorable to both cation and anion mobility. Under the assumption that ion association is comparable and of small magnitude in both PPO and PEO concentrated electrolytes,[22] the beneficial effect due to the lower binding energy in PPO is apparently overwhelmed by the detrimental effect due to its greater $T_g$ elevation. This, together with the microphase separation that takes place in PPO, could explain why PPO electrolytes are considerably less conductive than PEO amorphous electrolytes of the same compositions.[24]

A last point concerns the compositional features of dilute PPO electrolytes. According to this study, these electrolytes would consist of complexed microdomains dispersed in a salt-free PPO matrix. Furthermore, it is likely that this feature also applies to other polyethers such as PMGE and PEO. The difference between these polyethers appears to lie in the size of the complexed microphase. The better the solvating power of the polymer, the smaller and more labile are the complexed regions in equilibrium with the salt-free polymer. If this description is correct, some change must be made in the theoretical picture of these electrolytes. Such compositional features should necessarily play a role in the conduction process. Note that microphase separation in polymer ionic systems is not unique to polyether electrolytes. Some flexible ionomers, such as styrene–alkali metal methacrylate random copolymers, also exhibit a second $T_g$ above a certain ion concentration in the dilute regime.[25] The occurrence of this $T_g$ has been attributed to the formation of clusters of ion-pair aggregates. These clusters would contain polymer segments of restricted mobility. This

description, including ion-pair aggregation, is reasonable since random ionomers mainly consist of nonsolvating monomer units. Polyether electrolytes belong to a very different class of material.

**Acknowledgment.** This work was supported by the Research Institute of Hydro-Quebec (IREQ) and the Natural Sciences and Engineering Research Council of Canada.

## References and Notes

(1) Armand, M. B.; Chabagno, J. M.; Duclot, M. J. In *Fast Ion Transport in Solids*; Vashishta, P., Mundy, J. N., Shenoy, G. K., Eds.; Elsevier North-Holland: New York, 1979; p 131.
(2) Gray, F. M. *Solid Polymer Electrolytes*; VCH Publishers: New York, 1991.
(3) Gauthier, M.; Armand, M.; Muller, D. In *Electroresponsive Molecular and Polymeric Systems*; Skotheim, T. A., Ed.; Marcel Dekker Inc.: New York, 1988; Vol. 1, p 41.
(4) Besner, S.; Prud'homme, J. *Macromolecules* **1989**, *22*, 3029.
(5) Dumont, M.; Boils, D.; Harvey, P. E.; Prud'homme, J. *Macromolecules* **1991**, *24*, 1791.
(6) Robitaille, C.; Marques, S.; Boils, D.; Prud'homme, J. *Macromolecules* **1987**, *20*, 3023.
(7) Teeters, D.; Stewart, S. L.; Svoboda, L. *Solid State Ionics* **1988**, *28–30*, 1054.
(8) Greenbaum, S. G.; Pak, Y. S.; Wintersgill, M. C.; Fontanella, J. J. *Solid State Ionics* **1988**, *31*, 241.
(9) Moacanin, J.; Cuddihy, E. F. *J. Polym. Sci., Part C* **1966**, *14*, 313.
(10) Besner, S. Ph.D. Thesis, University of Montreal, 1992.
(11) Vallée, A.; Besner, S.; Prud'homme, J. *Electrochim. Acta* **1992**, *37*, 1579.
(12) Alamgir, M.; Moulton, R. D.; Abraham, K. M. *Electrochim. Acta* **1991**, *36*, 773.
(13) Torell, L. M.; Schantz, S. In *Polymer Electrolyte Reviews*; MacCallum, J. R., Vincent, C. A., Eds.; Elsevier Applied Science: New York, 1989; Vol. 2, p 1.
(14) Schantz, S. *J. Chem. Phys.* **1991**, *94*, 6296.
(15) McLin, M. G.; Angell, C. A. *J. Phys. Chem.* **1991**, *95*, 9464.
(16) Denault, J.; Morèse-Séguéla, B.; Séguéla, R.; Prud'homme, J. *Macromolecules* **1990**, *23*, 4658.
(17) Petrucci, S.; Eyring, E. M. *J. Phys. Chem.* **1991**, *95*, 1731.
(18) MacCallum, J. R.; Tomlin, A. S.; Vincent, C. A. *Eur. Polym. J.* **1986**, *22*, 787.
(19) Gray, F. M. *Solid State Ionics* **1990**, *40/41*, 637.
(20) Wunderlich, B. In *Thermal Characterization of Polymeric Materials*; Turi, E. A., Ed.; Academic Press: New York, 1981, p 81.
(21) Due to their high crystallization rate, PEO and PEO-rich mixtures (EO/salt > 32) could not be supercooled by melt quenching in the DSC apparatus. In its quenched form, the present, low molecular weight PEO did not exhibit any $T_g$ anomaly. Minor $T_g$ anomalies could be recorded over the range from −60 to −50 °C on quenched, high molecular weight PEO's, but these anomalies are not representative of a homogeneous, amorphous material.
(22) Besner, S.; Vallée, A.; Bouchard, G.; Prud'homme, J. *Macromolecules* **1992**, *25*, 6480.
(23) Papke, B. L.; Ratner, M. A.; Shriver, D. F. *J. Electrochem. Soc.* **1982**, *129*, 1694.
(24) For instance, over the ranges $50 < T < 100$ °C and $8 < O/Li < 40$, the conductivity data reported in ref 11 for solutions of $LiClO_4$ in amorphous PEO are greater by more than an order of magnitude than those reported in ref 15 for solutions of the same salt in PPO.
(25) Hird, B.; Eisenberg, A. *J. Polym. Sci., Polym. Phys. Ed.* **1990**, *28*, 1665.